

Spin squeezing a cold molecule

M. Bhattacharya

School of Physics and Astronomy, Rochester Institute of Technology, 84 Lomb Memorial Drive, Rochester, New York 14623, USA

(Received 12 September 2015; published 14 December 2015)

In this article we present a concrete proposal for spin squeezing the cold ground-state polar paramagnetic molecule OH, a system currently under fine control in the laboratory. In contrast to existing work, we consider a single, noninteracting molecule with angular momentum greater than $1/2$. Starting from an experimentally relevant effective Hamiltonian, we identify an adiabatic regime where different combinations of static electric and magnetic fields can be used to realize the single-axis twisting Hamiltonian of Kitagawa and Ueda [M. Kitagawa and M. Ueda, *Phys. Rev. A* **47**, 5138 (1993)], the uniform field Hamiltonian proposed by Law *et al.* [C. K. Law, H. T. Ng, and P. T. Leung, *Phys. Rev. A* **63**, 055601 (2001)], and a model of field propagation in a Kerr medium considered by Agarwal and Puri [G. S. Agarwal and R. R. Puri, *Phys. Rev. A* **39**, 2969 (1989)]. We then consider the situation in which nonadiabatic effects are quite large and show that the effective Hamiltonian supports spin squeezing even in this case. We provide analytical expressions as well as numerical calculations, including optimization of field strengths and accounting for the effects of field misalignment. Our results have consequences for applications such as precision spectroscopy, techniques such as magnetometry, and stereochemical effects such as the orientation-to-alignment transition.

DOI: [10.1103/PhysRevA.92.063823](https://doi.org/10.1103/PhysRevA.92.063823)

PACS number(s): 42.50.Dv, 42.50.Lc, 32.60.+i

I. INTRODUCTION

The cold OH molecule is a versatile platform for precision measurements. Its experimental appeal lies in the fact that its ground $X^2\Pi_{3/2}$ state is polar as well as paramagnetic and is therefore readily manipulated in the laboratory with the use of electric and magnetic fields [1–5]. Applications explored thus far include precision spectroscopy [6,7] and quantum information processing [8], in addition to studies of cold chemistry [9–13] and quantum degeneracy [14].

In this article, we consider spin squeezing of the OH molecule. Our discussion occurs in the context of the Heisenberg uncertainty relation [15]

$$\Delta J_x \Delta J_y \geq |\langle J_z \rangle|/2, \quad (1)$$

between the three components of the angular momentum operator J . Spin squeezing refers to a situation where the fluctuation in one of the components, say ΔJ_x , is reduced to below the standard quantum limit $\sqrt{|\langle J_z \rangle|/2}$. Of course, the fluctuations in J_y increase correspondingly, in order to maintain the relation of Eq. (1).

Spin squeezing constitutes a technique of interest at the frontiers of precision measurement and has applications in spectroscopy, magnetometry, metrology, the detection of particle correlation and entanglement, and quantum computation and simulation ([15,16] and references therein). The pioneering start to spin squeezing was provided by the work of Kitagawa and Ueda [17,18] and Wineland *et al.* [19,20], who considered the squeezing of collective atomic spins, and was followed by many investigations ([21–59], for example). We emphasize that all of this work relates to ensembles of correlated (pseudo)spins, represented by atoms (in a thermal vapor or a degenerate gas), nuclei [60], or molecules [61], where the collective spin can assume a high value [62].

More recently, squeezing has also been considered for single (atomic or nuclear) spins or, equivalently, for an uncorrelated ensemble of such spins. Experiments have been carried out, using spin-3 [63] and spin- $\frac{7}{2}$ [64] states of cesium

atoms. Possibilities also exist for dysprosium which offers states with spins from 8 up to 12.5. Theoretical calculations of single-spin squeezing have been presented as well [65]. The squeezing in this case is limited by the much smaller angular momentum available. Nonetheless, some effects can be experimentally relevant, for example, for precision spectroscopy [20]. Motivated by such a consideration, we consider spin squeezing of a single OH molecule. Interesting applications to the measurement of magnetic fields also seem possible [66–70], especially following recent discussions of magnetometry using single SiC spins with angular momentum $\frac{3}{2}$ [71]; ground-state cold OH also carries rotational angular momentum $\frac{3}{2}$ and is sensitive to magnetic fields via the Zeeman shift. Also, spin squeezing is related to the alignment-to-orientation transition [65], and we expect this perspective will be of relevance to our work, given the recent interest in the stereochemical properties of the OH molecule [72]. We emphasize that compared to previous proposals for spin squeezing molecules [61], which employ spin- $\frac{1}{2}$ interacting molecules squeezed collectively, we consider a single noninteracting molecule with angular momentum $\frac{3}{2}$.

In present-day laboratories, cold OH molecules are typically confined in magnetoelectrostatic traps [3,4,14,73,74]. We therefore consider spin squeezing enabled by these readily available static electric and magnetic fields. The advantage of using static, rather than optical or microwave [15], fields for squeezing is that damping and decoherence due to spontaneous emission can be avoided. Our starting point will be an effective eight-dimensional matrix Hamiltonian that has been shown to model recent OH experiments quite well [14,73,74] and has also been diagonalized analytically [75,76]. To obtain some physical intuition into this Hamiltonian, we first consider the regime in which Zeeman and Stark shifts are small compared to the Λ -doublet splitting of the OH ground state. We show that in this case an adiabatic Hamiltonian can be derived, which yields spin squeezing of the types considered earlier by Kitagawa and Ueda [18], Law *et al.* [30], and Agarwal and Puri [21]. Subsequently, we show that spin squeezing survives even in

the presence of large nonadiabatic effects implied by currently available experimental parameters. In fact, in some cases, the presence of nonadiabaticity introduces spin squeezing not present in the adiabatic model. We provide analytic and numerical results, discuss the optimization of the field strengths, and include the effects of field misalignment in our treatment.

The remainder of this article is arranged as follows. Section II presents the derivation of the adiabatic Hamiltonian, Sec. III discusses the dynamics of the squeezing parameter, Sec. IV addresses the detection of the proposed squeezing, and Sec. V supplies a conclusion.

II. DERIVATION OF THE ADIABATIC HAMILTONIAN

A. The eight-dimensional effective Hamiltonian

Several experiments on cold OH molecules in crossed electric and magnetic fields (see Fig. 1) have been successfully modeled using an effective Hamiltonian involving only eight quantum states [73,74]. The domain of validity of this Hamiltonian and the details of the states involved can be found in several articles [4,14,74,76] and are not repeated here. This effective Hamiltonian was recently diagonalized analytically following the detection of an underlying chiral symmetry [75]. In the process of identifying that symmetry, it was found that the OH matrix Hamiltonian could be reexpressed in terms of two interacting spins (to avoid notational clutter we set $\hbar = 1$; to make contact with laboratory parameters, requisite factors of \hbar can be supplied to any formula in this article by inspection, see the example supplied below),

$$H_M = -\tilde{\Delta}\sigma_z - \tilde{B}J_z + \tilde{E}\sigma_x(J_z \cos \theta - J_x \sin \theta), \quad (2)$$

where the constants are given by

$$\tilde{\Delta} = \frac{\Delta}{2}, \quad \tilde{B} = \frac{4\mu_B B}{5}, \quad \tilde{E} = \frac{2\mu_e E}{5}, \quad (3)$$

Δ being the Λ -doublet splitting, B and E the uniform magnetic and electric fields, respectively, μ_B the Bohr magneton, and μ_e the electric dipole moment of the OH molecule. In Eq. (2),

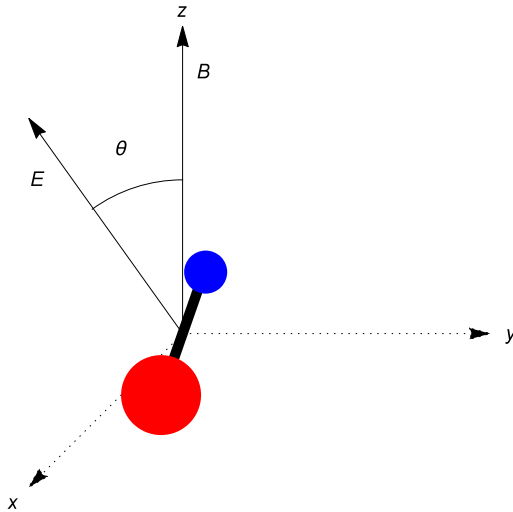


FIG. 1. (Color online) Schematic of the diatomic OH molecule in electric, E , and magnetic, B , fields crossed at the angle θ .

θ is the angle between the electric and magnetic fields (see Fig. 1), and $\sigma = \frac{1}{2}$ and $J = \frac{3}{2}$ are the two interacting spins. The spin σ is a pseudospin, with the projections $\sigma_z = -1$ and $\sigma_z = 1$ corresponding to the two Λ -doublet manifolds of parity e and f , respectively. On the other hand, J corresponds to the rotation of the molecular axis, and the values $J_z = \pm\frac{1}{2}$ and $\pm\frac{3}{2}$ indicate the various projections of J on the laboratory z axis, which is chosen for convenience and without loss of generality to be along the magnetic field. The matrix representation of H_M is reproduced in the appendix for the reader's convenience [see Eq. (A1)].

At this point the insertion of factors of \hbar in Eq. (2) may be considered as a useful exercise. We begin with the observation that H_M has units of energy. Since the Pauli matrix σ_x is dimensionless, $\tilde{\Delta}$ needs to have units of energy and thus must be multiplied by \hbar . On the other hand, J_z has units of \hbar . Therefore \tilde{B} needs to have units of frequency, and thus the right-hand side of the corresponding expression in Eq. (3) must be divided by an \hbar . Other formulas in this article can be handled in a similar manner.

B. The four-dimensional adiabatic Hamiltonian

The generation of spin squeezing requires the presence of a nonlinearity, represented to lowest order by a term quadratic in one of the spin operators in the relevant Hamiltonian [18]. However, Eq. (2) is linear in each of the spin operators. It may not be readily obvious that the coupled dynamics of the two spins can lead to squeezing, and it would assist our intuition if H_M could be reduced, even if in some restricted regime, to the form of a spin-squeezing Hamiltonian familiar from the literature. In order to effect such a reduction, we proceed by identifying a regime in which the pseudospin- $\frac{1}{2}$ can be eliminated adiabatically. As we show below, this results in an effective spin-squeezing Hamiltonian for the spin- $\frac{3}{2}$ degree of freedom. A similar procedure has been used earlier in the case of nuclear spin squeezing; in that case, however, the eliminated spin is real [60].

The derivation begins with the Heisenberg equations implied by Eq. (2) for the system variables:

$$\dot{\sigma}_x = 2\tilde{\Delta}\sigma_y, \quad (4)$$

$$\dot{\sigma}_y = -2\tilde{\Delta}\sigma_x - 2\tilde{E}\sigma_z(J_z \cos \theta - J_x \sin \theta), \quad (5)$$

$$\dot{\sigma}_z = 2\tilde{E}\sigma_y(J_z \cos \theta - J_x \sin \theta), \quad (6)$$

$$\dot{J}_x = \tilde{B}J_y - \tilde{E} \cos \theta \sigma_x J_y, \quad (7)$$

$$\dot{J}_y = -\tilde{B}J_x + \tilde{E}\sigma_x(J_x \cos \theta + J_z \sin \theta), \quad (8)$$

$$\dot{J}_z = -\tilde{E} \sin \theta \sigma_x J_y. \quad (9)$$

We now consider the regime

$$\tilde{\Delta} > \tilde{E}, \tilde{B}, \quad (10)$$

i.e., such that the Λ -doublet splitting is larger than the Stark as well as the Zeeman shifts. In the regime indicated by Eq. (10),

σ_x and σ_y will vary at the high rate $\sim 2\tilde{\Delta}$ and may be thought of as the “fast” variables of our problem. We see below that with this assumption σ_z ceases to be a dynamical variable, i.e., takes on a constant value. On the other hand, J_x , J_y , and J_z , varying at the low rates $\sim \tilde{B}$ and $\sim \tilde{E}$ (to first order), may be thought of as the “slow” variables of the problem. We now adiabatically eliminate the fast spin variables σ_x and σ_y in Eqs. (4) and (5) by setting the time derivatives in those equations equal to zero. The resulting solutions are

$$\sigma_x = -\frac{\tilde{E}C}{\tilde{\Delta}}(J_z \cos \theta - J_x \sin \theta), \quad (11)$$

$$\sigma_y = 0, \quad (12)$$

$$\sigma_z = C, \quad (13)$$

where C can take the values ± 1 . Note that the adiabatic solution $\sigma_y = 0$ forces σ_z to be a constant [see Eq. (6)], as mentioned above. We now use the solutions of Eqs. (11)–(13) to adiabatically eliminate the fast spin 1/2 degrees of freedom from Eq. (2). Dropping a constant term proportional to $\tilde{\Delta}$, we obtain the adiabatic Hamiltonian for the spin- $\frac{3}{2}$ variables

$$H_a = -\tilde{B}J_z - \frac{C\tilde{E}^2}{\tilde{\Delta}}(J_z \cos \theta - J_x \sin \theta)^2, \quad (14)$$

which clearly contains terms nonlinear in the angular momentum components and can therefore enforce squeezing.

We note that the separation of variables into slow and fast groups becomes more rigorous as $(\tilde{E}/\tilde{\Delta}, \tilde{B}/\tilde{\Delta}) \rightarrow 0$. In our calculations below we work with $\tilde{E}/\tilde{\Delta} \simeq 0.25$, which corresponds to an electric field of 100 V/cm, the lower bound stipulated by the value of stray fields currently affecting experiments [74]. We also consider $\tilde{B}/\tilde{\Delta} \leq 0.1$, corresponding to a magnetic field of 20 G, which can easily be achieved experimentally. These parameter values place us in the adiabatic, but not *deep* adiabatic, regime. However, such a distinction is not critical, since as we show later in this article, spin squeezing exists in OH even in the presence of quite large nonadiabatic effects, which can, in fact, in some cases introduce squeezing not anticipated by the adiabatic approximation. The derivation of the adiabatic Hamiltonian of Eq. (14) serves the purpose of providing some intuition for the existence of spin squeezing in the system and provides a benchmark for determining how large the nonadiabatic effects are in the spin-squeezing dynamics. Of course, future OH experiments can be designed with even smaller fields for which the adiabatic approximation improves. See, for example, compensation techniques that have been used to limit stray electric fields to about 1 V/cm already in other systems [77].

Below, we show that some standard squeezing Hamiltonians can be recovered from Eq. (14) and also explore the squeezing effects of this Hamiltonian for arbitrary \tilde{B} , \tilde{E} , and θ , within the limits prescribed by the validity of the effective Hamiltonian [Eq. (2)]. Subsequently, we compare these results with numerical calculations based on the full eight-dimensional Hamiltonian of Eq. (2), which accounts for nonadiabatic effects. We note that Eq. (10) does not stipulate any relationship between \tilde{E} and \tilde{B} , other than that they both

have to be smaller than $\tilde{\Delta}$. We use this flexibility below to adjust the field magnitudes to optimize squeezing.

III. SPIN-SQUEEZING DYNAMICS

A. Spin squeezing using the four-dimensional adiabatic Hamiltonian H_a

In this section we consider spin squeezing using the four-dimensional adiabatic Hamiltonian of Eq. (14). We provide analytic and numerical results, as appropriate.

1. One-axis twisting

For $\tilde{B} = 0$, $\theta = 0$, and $C = 1$, Eq. (14) gives the Kitagawa-Ueda Hamiltonian [18],

$$H_{\text{KU}} = \tilde{\kappa} J_z^2, \quad (15)$$

where

$$\tilde{\kappa} = -\frac{\tilde{E}^2}{\tilde{\Delta}}. \quad (16)$$

The theoretical analysis for spin squeezing using H_{KU} was first provided by Kitagawa and Ueda [18] and more recently by Rochester *et al.* [65]. Nonetheless, we restate the procedure here, in order to compare with fully numerical calculations to be presented later. The recipe for the analysis is as follows. Using the four-dimensional matrix for the $J = \frac{3}{2}$ operator J_z [78], we write the matrix form for H_{KU} . We then obtain the time evolution operator

$$U_{\text{KU}} = e^{-iH_{\text{KU}}t}, \quad (17)$$

which is also a four-dimensional matrix. We can then obtain the time evolution of any observable \mathcal{O} by using the relation $\mathcal{O}(t) = U_{\text{KU}}^{-1} \mathcal{O} U_{\text{KU}}$. In this way we find the matrix forms of the observables $J_x(t)$ and $J_y(t)$. In order to find the most suitable axis for spin squeezing, it is convenient to consider a further rotation by an angle, n , about the x axis [18], i.e.,

$$J_{y,n}(t) = e^{inJ_x(t)} J_y(t) e^{-inJ_x(t)}, \quad (18)$$

and so on for other observables. The operators $J_x(t)$ and $J_x^2(t)$ are unaffected by this rotation, of course.

For our initial state, we choose, following Kitagawa and Ueda, the (coherent) stretched state along the x axis [18],

$$|i\rangle_{\text{KU}} = \left| J = \frac{3}{2}, M = \frac{3}{2} \right\rangle_{\hat{x}} = 2^{-3/2} \sum_{k=0}^3 \binom{3}{k} \left| \frac{3}{2}, \frac{3}{2} - k \right\rangle, \quad (19)$$

which we have expanded in the z basis on the right-hand side. We note that the current level of control over the OH ground-state manifold should readily allow this state to be prepared [74]. Using the initial state $|i\rangle_{\text{KU}}$ we find the expectation values $\langle J_{y,n}(t) \rangle$, $\langle J_{y,n}^2(t) \rangle$, etc., and thence the variances such as

$$[\Delta J_{y,n}(t)]^2 = \langle J_{y,n}^2(t) \rangle - \langle J_{y,n}(t) \rangle^2. \quad (20)$$

This procedure yields the relevant quantities [65]

$$\langle J_x(t) \rangle = \frac{3}{2} \cos^2 \tilde{\kappa} t, \quad (21)$$

$$[\Delta J_{y,n}(t)]^2 = \frac{3}{4} \left[1 + \frac{M}{2} + \frac{\sqrt{M^2 + N^2}}{2} \cos(2n + 2\delta) \right],$$

$$[\Delta J_{z,n}(t)]^2 = \frac{3}{4} \left[1 + \frac{M}{2} - \frac{\sqrt{M^2 + N^2}}{2} \cos(2n + 2\delta) \right], \quad (22)$$

where

$$M = 1 - \cos 2\tilde{\kappa} t, \quad N = 2 \sin 2\tilde{\kappa} t, \quad \delta = \frac{1}{2} \tan^{-1} \left(\frac{N}{M} \right). \quad (23)$$

As pointed out earlier [18,65], the y quadrature is maximally squeezed for $\cos(2n_{\text{opt}} + 2\delta) = -1$, i.e., along the axis

$$n_{\text{opt}} = \frac{\pi}{2} - \delta, \quad (24)$$

in the y - z plane. The amount of squeezing is quantified by the parameter introduced by Wineland *et al.* [20],

$$\xi_{y,n} = \sqrt{3} \frac{\langle (\Delta J_{y,n}(t)) \rangle}{|\langle J_x(t) \rangle|}, \quad (25)$$

and, analogously,

$$\xi_{z,n} = \sqrt{3} \frac{\langle (\Delta J_{z,n}(t)) \rangle}{|\langle J_x(t) \rangle|}. \quad (26)$$

Squeezing occurs when either $\xi_{y,n}$ or $\xi_{z,n}$ is less than one. We have shown a plot of $\xi_{y,n_{\text{opt}}}$ in Fig. 2. The blue (dashed) line is the analytical prediction from Eqs. (24) and (25) based on the adiabatic approximation of Eq. (10), with $\tilde{E}/\tilde{\Delta} \simeq 0.25$. The red (solid) curve is the numerical calculation using the eight-dimensional effective Hamiltonian of Eq. (2). As can be seen, nonadiabatic effects are quite large and significantly change the magnitude and periodicity of the squeezing, which is nonetheless present.

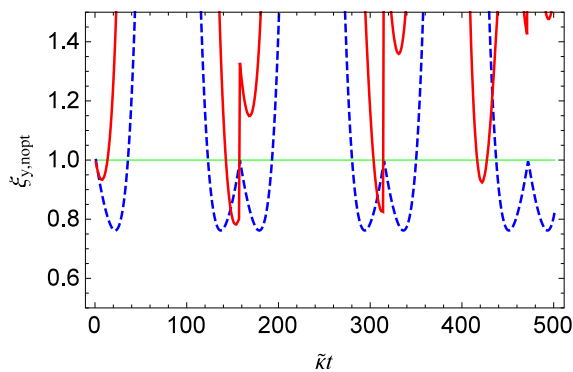


FIG. 2. (Color online) Plot of $\xi_{y,n_{\text{opt}}}$ as a function of the dimensionless time $\tilde{\kappa} t$, where $\tilde{\kappa}$ is defined in Eq. (16). The parameters are $\Delta = 1.66$ GHz, $E = 100$ V/cm, and $B = 0$, implying $\tilde{\kappa} = 48$ MHz. Squeezing occurs when $\xi_{y,n_{\text{opt}}} < 1$. The blue (dashed) curve is the analytical prediction from Eqs. (24) and (25) based on the adiabatic approximation of Eq. (10), with $\tilde{E}/\tilde{\Delta} \simeq 0.25$. The red (solid) curve is the numerical calculation using the eight-dimensional effective Hamiltonian of Eq. (2). As can be seen, nonadiabatic effects are quite large and significantly change the magnitude and periodicity of the squeezing, which is nonetheless present.

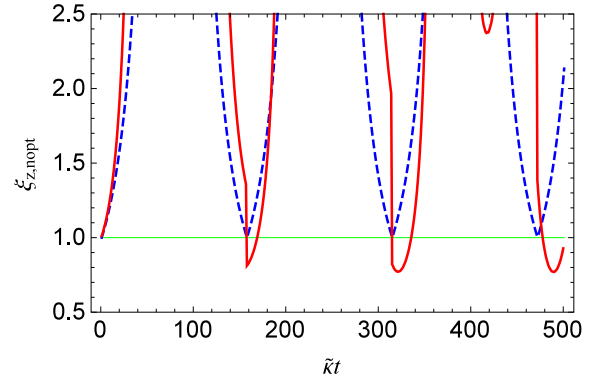


FIG. 3. (Color online) Plot of $\xi_{z,n_{\text{opt}}}$ as a function of the dimensionless time $\tilde{\kappa} t$, where $\tilde{\kappa}$ is defined in Eq. (16). The parameters are $\Delta = 1.66$ GHz, $E = 100$ V/cm, and $B = 0$, implying $\tilde{\kappa} = 48$ MHz. Squeezing occurs when $\xi_{z,n_{\text{opt}}} < 1$. The blue (dashed) curve is the analytical prediction from Eqs. (24) and (26) based on the adiabatic approximation of Eq. (10), with $\tilde{E}/\tilde{\Delta} \simeq 0.25$. The red (solid) curve is the numerical calculation using the eight-dimensional effective Hamiltonian of Eq. (2). As can be seen, nonadiabatic effects are noticeable and actually introduce some squeezing into the otherwise “antisqueezed” quadrature.

The red (solid) curve in Fig. 2 corresponds to a numerical calculation of squeezing using the full effective Hamiltonian of Eq. (2), which incorporates the effects of nonadiabaticity (see Sec. III B below). As can be seen, although there are qualitative similarities between the solid and dashed curves (such as the periodic presence of minima), the adiabatic approximation is not very good, and nonadiabatic effects change the magnitude and periodicity of squeezing quite significantly. This may be expected, as our adiabaticity parameter $\tilde{E}/\tilde{\Delta} \sim 0.25$ is not very small. However, as mentioned above, the badness of the adiabatic approximation is not a matter of concern, since our aim is rather to locate spin squeezing of OH, which indeed persists even in the presence of large nonadiabaticity.

A plot of $\xi_{z,n_{\text{opt}}}$ has been shown in Fig. 3. The analytical prediction of Eq. (26), represented by the blue (dashed) curve, implies that the shown z quadrature is never squeezed. Interestingly, the proper inclusion of nonadiabatic effects, shown by the red (solid) curve, introduces some squeezing of this quadrature.

2. Uniform field Hamiltonian

In this section we consider spin squeezing in the presence of a magnetic field. For $\tilde{B} \neq 0$, and $\theta = \frac{\pi}{2}$, Eq. (14) takes the form

$$H_{\text{LNL}} = -\tilde{B} J_z + \tilde{\kappa} J_x^2. \quad (27)$$

This Hamiltonian is, to within a unitary anticlockwise rotation of $\frac{\pi}{2}$ around the y axis, the same as that proposed earlier by Law, Ng, and Leung [30,79–81]. These authors suggested adding the uniform field term to the Kitagawa-Ueda Hamiltonian as it yielded greater squeezing for longer times. Analytic solutions to the spin-squeezing dynamics of Eq. (27) are not available for arbitrary spin J . Generally, analytic results can be found only for $J \leq 2$, since the eigenvalues of the Hamiltonian are required for the calculation, which can be

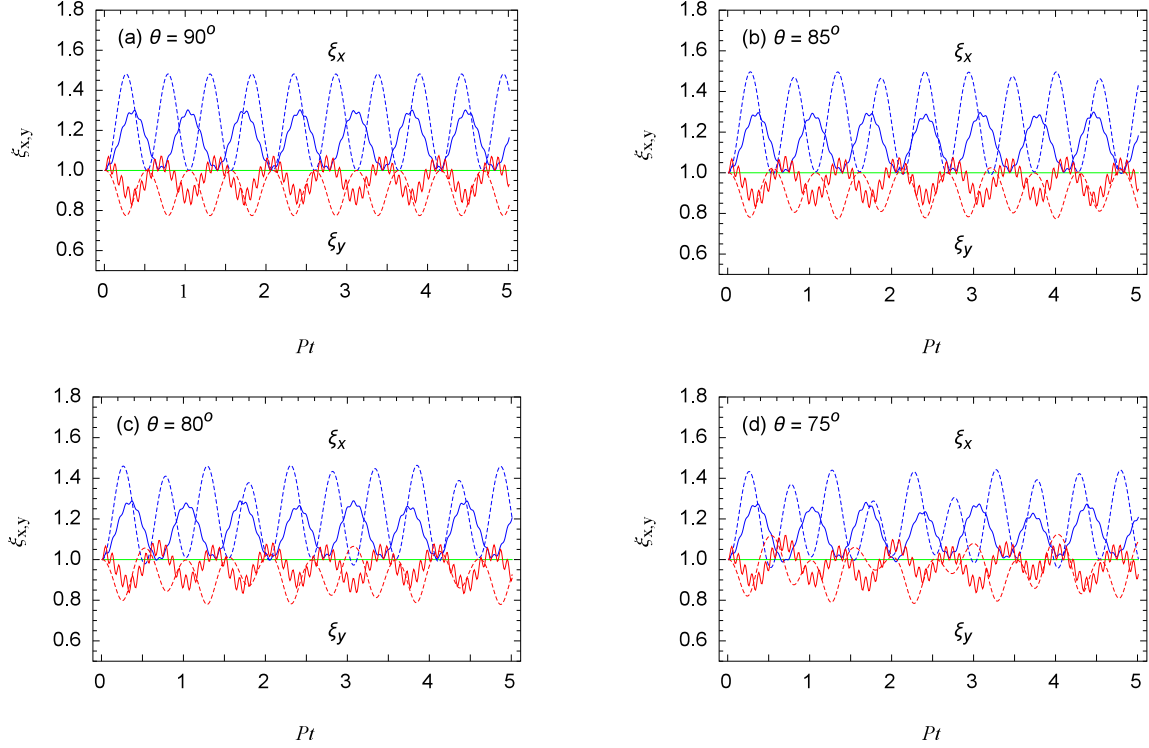


FIG. 4. (Color online) Plots of $\xi_{x,y}$ as functions of the dimensionless time Pt , where P is defined in Eq. (33). The parameters are $\Delta = 1.66$ GHz, $E = 100$ V/cm, $B = 20$ G, implying $P = 144$ MHz and (a) $\theta = 90^\circ$, (b) $\theta = 85^\circ$, (c) $\theta = 80^\circ$, and (d) $\theta = 75^\circ$. Squeezing occurs when $\xi_{x,y} < 1$. The dashed curves are the analytical predictions for ξ_x [Eq. (34)] (blue) and ξ_y [Eq. (35)] (red). The solid curves represent numerical calculations carried out using the eight-dimensional effective Hamiltonian of Eq. (2). As can be seen by comparing with Fig. 2, the presence of squeezing is quite robust to nonadiabatic effects. Also, deviations of about 5° away from the nominal value of 90° for field alignment do not affect the squeezing greatly.

found in closed form only for matrices of dimension 5 or lower. Some results for the case where $J = \frac{3}{2}$ is a collective spin have been published in the literature [81,82]. We provide additional expressions in order to discuss the details of our problem.

To determine the squeezing, we follow a procedure similar to that of Sec. III A 1, but consider the initial stretched state along the z direction,

$$|i\rangle_{\text{LNL}} = |0,0,0,1\rangle, \quad (28)$$

and determine the squeezing about the x and y axes. We find

$$\langle J_x(t) \rangle = \langle J_y(t) \rangle = 0, \quad (29)$$

$$\langle J_z(t) \rangle = \frac{3}{2} \left[1 - \left(\frac{\tilde{\kappa}}{P} \sin Pt \right)^2 \right], \quad (30)$$

$$\langle [\Delta J_x(t)]^2 \rangle = \frac{3}{4} \left[1 + 2\tilde{\kappa}\tilde{B} \left(\frac{\sin Pt}{P} \right)^2 \right], \quad (31)$$

$$\langle [\Delta J_y(t)]^2 \rangle = \frac{3}{4} \left[1 - 2\tilde{\kappa}(\tilde{B} - \tilde{\kappa}) \left(\frac{\sin Pt}{P} \right)^2 \right], \quad (32)$$

where

$$P = \sqrt{\tilde{B}^2 - \tilde{B}\tilde{\kappa} + \tilde{\kappa}^2}. \quad (33)$$

Using Eqs. (29)–(32), we can find the squeezing parameters

$$\xi_x = \sqrt{3} \frac{\langle [\Delta J_x(t)] \rangle}{|\langle J_z(t) \rangle|} \quad (34)$$

and

$$\xi_y = \sqrt{3} \frac{\langle [\Delta J_y(t)] \rangle}{|\langle J_z(t) \rangle|}. \quad (35)$$

Plots of the squeezing dynamics are shown in Fig. 4(a) for the same parameters as in Fig. (2) but with $B = 20$ G. The dashed curves represent the analytical results for ξ_x [Eqs. (34)] (blue) and ξ_y [Eq. (35)] (red). The solid curves are the corresponding numerical calculations using H_M from Eq. (2). It can be seen by comparing Fig. 4(a) to Figs. 2 and 3 that the Law-Ng-Leung approach is more robust to nonadiabatic effects than the Kitagawa-Ueda model. More specifically, as can be seen from Figs. 2 and 3, the presence of nonadiabatic effects (solid line) changes the spin-squeezing dynamics from the predictions of the adiabatic Hamiltonian (dashed line) quite considerably. These changes involve both the magnitude and the periodicity of the squeezing; in fact the squeezing becomes rather erratic in the presence of nonadiabatic effects. In contrast, the presence of nonadiabatic effects (solid lines) does not make the squeezing very erratic in Fig. 4(a), although the adiabatic approximation is still not very good. In that figure, the nonadiabatic squeezing has an amplitude similar to the adiabatic prediction (dashed lines), especially for ξ_y .

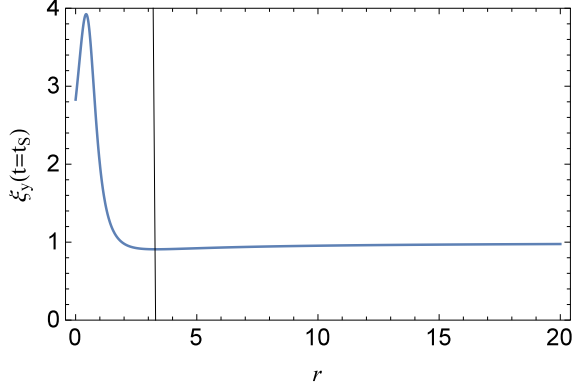


FIG. 5. (Color online) Plot of $\xi_y(t = t_S)$ [Eq. (37)] versus r [Eq. (38)]. The vertical line corresponds to $r \simeq 3.3$, at which $\xi_y(t = t_S)$ has a minimum, corresponding to maximum squeezing.

The time period is also quite regular and close to that of the adiabatic case. The main difference from the adiabatic case is the presence of fast modulations appearing due to the presence of nonadiabatic effects.

In Fig. 4 we have chosen a magnetic field optimized using the following procedure. From the analytic result of Eq. (35), it can be seen that at multiples of the time t_S ,

$$t_S = \frac{\pi}{4P}, \quad (36)$$

the squeezing parameter for the y quadrature attains an extremum value given by

$$\xi_y(t = t_S) = \frac{2\sqrt{(r^2 - r + 1)(r^2 - 2r + 2)}}{2r^2 - 2r + 1}, \quad (37)$$

where the dimensionless ratio

$$r = \frac{\tilde{B}}{|\tilde{\kappa}|}. \quad (38)$$

The denominator of $\xi_y(t = t_S)$ vanishes only for the complex values $r = (1 \pm i)/2$, which are excluded by experiment. Thus, ξ_y^{\min} stays finite as r varies, as can be seen from Fig. 5.

Differentiation of Eq. (37) readily yields a minimum value, $\xi_y^{\min}(t = t_S) \simeq 0.8$, which occurs at $r \simeq 3.3$, indicated by the vertical line in Fig. 5. This optimized value of r corresponds to the magnetic field 20 G used in Fig. 4(a). For simplicity, unlike in Ref. [81], we have not found the time-dependent axis of optimum squeezing, which can lead to even better squeezing than we have presented.

3. General case

In this section we consider spin squeezing as a function of the angle between the electric and magnetic fields. The interest in this degree of freedom arises from the necessity of accounting for possible misalignments between the electric and magnetic fields in the laboratory, e.g., away from the nominal value of $\theta = \frac{\pi}{2}$ for H_{LNL} (see Sec. III A 2). While this case can be solved analytically as well, the expressions are lengthy and we provide numerical solutions instead. The

Hamiltonian is

$$H_g = -\tilde{B}J_z + \tilde{\kappa}(J_z \cos \theta - J_x \sin \theta)^2. \quad (39)$$

Before we proceed further, we mention that this Hamiltonian, when rotated anticlockwise by an angle θ about the y axis yields

$$H'_g = e^{i\theta J_y} H_g e^{-i\theta J_y} = -\tilde{B}(J_z \cos \theta - J_x \sin \theta) + \tilde{\kappa} J_z^2, \quad (40)$$

which is of the form considered earlier by Agarwal and Puri for arbitrary J [21].

Numerical plots are presented in Fig. 4 for (b) $\theta = 85^\circ$, (c) $\theta = 80^\circ$, and (d) $\theta = 75^\circ$, respectively. The dashed curves are the numerical implications of Eq. (39) for ξ_x [Eq. (34)] (blue) and ξ_y [Eq. (35)] (red). The solid curves are the corresponding numerical calculations starting from Eq. (2). As can be seen, the squeezing is quite robust to field misalignment, meaning that Figs. 4(b) and 4(c) do not vary too much from Fig. 4(a). Only at about $\theta = 75^\circ$ does the pattern change noticeably from that at $\theta = 90^\circ$. Interestingly, while misalignment degrades squeezing in the y quadrature, it does not correspondingly introduce squeezing in the x quadrature.

B. Spin squeezing using the eight-dimensional effective Hamiltonian H_M

In this section we give the details of our spin-squeezing calculations using the full eight-dimensional Hamiltonian H_M of Eq. (2). We begin with the eight-dimensional matrix representation of H_M from Eq. (A1). Although the treatment can be carried out analytically, the expressions are very long, and we calculate instead numerically the time-evolution operator

$$U_M = e^{-iH_M t}, \quad (41)$$

which is also an eight-dimensional matrix. Starting from the initial state $|\psi(0)\rangle$, represented by an eight-dimensional column matrix, the state vector $|\psi(t)\rangle$ at any later time t is

$$|\psi(t)\rangle = U_M |\psi(0)\rangle. \quad (42)$$

The density matrix of the full system can then be easily found:

$$\rho(t) = |\psi(t)\rangle \langle \psi(t)|. \quad (43)$$

The reduced density matrix of the spin- $\frac{3}{2}$ system can then be found by tracing over the spin- $\frac{1}{2}$ degrees of freedom, i.e.,

$$\rho_{3/2}(t) = \text{Tr}_{1/2}[\rho(t)]. \quad (44)$$

From here the expectation values of the relevant operators can be calculated, such as

$$\langle J_x(t) \rangle = \text{Tr}_{3/2}[J_x \rho_{3/2}(t)], \quad (45)$$

and therefore also the squeezing parameters, as for example in Eq. (34). It may be useful to mention that for Sec. III A 1 the initial state is now written as

$$|i\rangle_{\text{KU}} = \frac{1}{2\sqrt{2}} |0,0,0,0,1,\sqrt{3},\sqrt{3},1\rangle, \quad (46)$$

and for Secs. III A 2 and III A 3 it is written as

$$|i\rangle_{\text{LNL}} = |0,0,0,0,0,0,1\rangle. \quad (47)$$

IV. DETECTION OF SPIN SQUEEZING

The proposed spin squeezing may be detected by performing quantum tomography on the OH ground-state manifold, which would yield the density matrix, from which squeezing information can readily be extracted. Such procedures can be carried out for OH in analogy to experiments performed earlier on atomic [63] and nuclear [64] systems. In the laboratory, the predicted squeezing will be degraded by damping and noise, due to molecular collisions and trap loss. In the present work, we have justifiably neglected these effects, since they occur at typical rates of Hz (collisions) [3,4,9] or kHz (trap loss) [74], while squeezing is generated at frequencies of MHz (see Fig. 2).

V. CONCLUSION

We have proposed a scheme for spin squeezing the cold OH molecule in the context of ongoing experiments. Production of such nonclassical states is expected to be useful for spectroscopy, magnetometry, and stereochemistry. We have identified a regime of adiabaticity where some intuition regarding spin squeezing in the system can be gathered. We have then shown that spin squeezing can be found even when nonadiabatic effects are large. Since we do not propose to

use optical or microwave fields, our scheme is free from damping and decoherence due to spontaneous emission and optical pumping. In our analysis, we have shown how to optimize the field values and have also investigated the effect of field misalignment on the squeezing. Our work is a concrete proposal for spin squeezing single noninteracting molecules with angular momentum greater than $\frac{1}{2}$. We note that with the use of additional electric and magnetic fields, other spin-squeezing Hamiltonians may also be realized using OH, such as the one proposed by Raghavan *et al.* [31]. Also, a more accurate description of the OH ground state can be reached by including more states in the Hamiltonian, accounting for fine and hyperfine structure and electric quadrupole interactions [4,83]. It would be interesting to investigate the effect of these additions on our results. Finally, our scheme can also be extended to the ground states of other polar paramagnetic molecules such as $^2\Pi_{3/2}$ LiO and $^3\Phi_2$ CeO.

ACKNOWLEDGMENTS

We thank S. Marin for useful discussions.

APPENDIX

In this Appendix we provide, for the reader's convenience, the matrix representation of H_M from Eq. (2) [73,75]:

$$H_M = \begin{pmatrix} -\frac{\hbar\Delta}{2} - \frac{6}{5}\mu_B B & 0 & 0 & 0 & \frac{3}{5}\mu_e E \cos\theta & -\frac{\sqrt{3}}{5}\mu_e E \sin\theta & 0 & 0 \\ 0 & -\frac{\hbar\Delta}{2} - \frac{2}{5}\mu_B B & 0 & 0 & -\frac{\sqrt{3}}{5}\mu_e E \sin\theta & \frac{1}{5}\mu_e E \cos\theta & -\frac{2}{5}\mu_e E \sin\theta & 0 \\ 0 & 0 & -\frac{\hbar\Delta}{2} + \frac{2}{5}\mu_B B & 0 & 0 & -\frac{2}{5}\mu_e E \sin\theta & -\frac{1}{5}\mu_e E \cos\theta & -\frac{\sqrt{3}}{5}\mu_e E \sin\theta \\ 0 & 0 & 0 & -\frac{\hbar\Delta}{2} + \frac{6}{5}\mu_B B & 0 & 0 & -\frac{\sqrt{3}}{5}\mu_e E \sin\theta & -\frac{3}{5}\mu_e E \cos\theta \\ \frac{3}{5}\mu_e E \cos\theta & -\frac{\sqrt{3}}{5}\mu_e E \sin\theta & 0 & 0 & \frac{\hbar\Delta}{2} - \frac{6}{5}\mu_B B & 0 & 0 & 0 \\ -\frac{\sqrt{3}}{5}\mu_e E \sin\theta & \frac{1}{5}\mu_e E \cos\theta & -\frac{2}{5}\mu_e E \sin\theta & 0 & 0 & \frac{\hbar\Delta}{2} - \frac{2}{5}\mu_B B & 0 & 0 \\ 0 & -\frac{2}{5}\mu_e E \sin\theta & -\frac{1}{5}\mu_e E \cos\theta & -\frac{\sqrt{3}}{5}\mu_e E \sin\theta & 0 & 0 & \frac{\hbar\Delta}{2} + \frac{2}{5}\mu_B B & 0 \\ 0 & 0 & -\frac{\sqrt{3}}{5}\mu_e E \sin\theta & -\frac{3}{5}\mu_e E \cos\theta & 0 & 0 & 0 & \frac{\hbar\Delta}{2} + \frac{6}{5}\mu_B B \end{pmatrix}. \quad (\text{A1})$$

- [1] J. R. Bochinski, E. R. Hudson, H. J. Lewandowski, G. Meijer, and J. Ye, *Phys. Rev. Lett.* **91**, 243001 (2003).
 [2] J. R. Bochinski, E. R. Hudson, H. J. Lewandowski, and J. Ye, *Phys. Rev. A* **70**, 043410 (2004).
 [3] S. Y. T. van de Meerakker, P. H. M. Smeets, N. Vanhaecke, R. T. Jongma, and G. Meijer, *Phys. Rev. Lett.* **94**, 023004 (2005).
 [4] B. C. Sawyer, B. L. Lev, E. R. Hudson, B. K. Stuhl, M. Lara, J. L. Bohn, and J. Ye, *Phys. Rev. Lett.* **98**, 253002 (2007).
 [5] M. Lemeshko, R. V. Krems, J. M. Doyle, and S. Kais, *Mol. Phys.* **111**, 1648 (2013).
 [6] E. R. Hudson, H. J. Lewandowski, B. C. Sawyer, and J. Ye, *Phys. Rev. Lett.* **96**, 143004 (2006).
 [7] M. G. Kozlov, *Phys. Rev. A* **80**, 022118 (2009).
 [8] B. L. Lev, E. R. Meyer, E. R. Hudson, B. C. Sawyer, J. L. Bohn, and J. Ye, *Phys. Rev. A* **74**, 061402(R) (2006).
 [9] A. V. Avdeenkov and J. L. Bohn, *Phys. Rev. A* **66**, 052718 (2002).
 [10] A. V. Avdeenkov and J. L. Bohn, *Phys. Rev. Lett.* **90**, 043006 (2003).
 [11] C. Ticknor and J. L. Bohn, *Phys. Rev. A* **71**, 022709 (2005).
 [12] B. C. Sawyer, B. K. Stuhl, D. Wang, M. Yeo, and J. Ye, *Phys. Rev. Lett.* **101**, 203203 (2008).
 [13] T. V. Tscherbul, Z. Pavlovic, H. R. Sadeghpour, R. Cote, and A. Dalgarno, *Phys. Rev. A* **82**, 022704 (2010).
 [14] B. K. Stuhl, M. T. Hummon, M. Yeo, G. Quemener, J. L. Bohn, and J. Ye, *Nature (London)* **492**, 396 (2012).
 [15] J. Ma, X. Wang, C. P. Sun, and F. Nori, *Phys. Rep.* **509**, 89 (2011).
 [16] C. Gross, *J. Phys. B* **45**, 103001 (2012).
 [17] M. Kitagawa and M. Ueda, *Phys. Rev. Lett.* **67**, 1852 (1991).

- [18] M. Kitagawa and M. Ueda, *Phys. Rev. A* **47**, 5138 (1993).
- [19] D. J. Wineland, J. J. Bollinger, W. M. Itano, F. L. Moore, and D. J. Heinzen, *Phys. Rev. A* **46**, R6797 (1992).
- [20] D. J. Wineland, J. J. Bollinger, W. M. Itano, and D. J. Heinzen, *Phys. Rev. A* **50**, 67 (1994).
- [21] G. S. Agarwal and R. R. Puri, *Phys. Rev. A* **39**, 2969 (1989).
- [22] G. S. Agarwal and R. R. Puri, *Phys. Rev. A* **41**, 3782 (1990).
- [23] A. Kuzmich, K. Molmer, and E. S. Polzik, *Phys. Rev. Lett.* **79**, 4782 (1997).
- [24] J. Hald, J. L. Sorensen, C. Schori, and E. S. Polzik, *Phys. Rev. Lett.* **83**, 1319 (1999).
- [25] A. Sorensen and K. Molmer, *Phys. Rev. Lett.* **83**, 2274 (1999).
- [26] A. Kuzmich, L. Mandel, and N. P. Bigelow, *Phys. Rev. Lett.* **85**, 1594 (2000).
- [27] H. Pu and P. Meystre, *Phys. Rev. Lett.* **85**, 3987 (2000).
- [28] L. M. Duan, A. Sorensen, J. I. Cirac, and P. Zoller, *Phys. Rev. Lett.* **85**, 3991 (2000).
- [29] L. Vernac, M. Pinard, and E. Giacobino, *Phys. Rev. A* **62**, 063812 (2000).
- [30] C. K. Law, H. T. Ng, and P. T. Leung, *Phys. Rev. A* **63**, 055601 (2001).
- [31] S. Raghavan, H. Pu, P. Meystre, and N. P. Bigelow, *Opt. Commun.* **188**, 149 (2001).
- [32] K. Helmerson and L. You, *Phys. Rev. Lett.* **87**, 170402 (2001).
- [33] A. Vardi and J. R. Anglin, *Phys. Rev. Lett.* **86**, 568 (2001).
- [34] A. S. Sorensen and K. Molmer, *Phys. Rev. Lett.* **86**, 4431 (2001).
- [35] L. Vernac, M. Pinard, V. Josse, and E. Giacobino, *Eur. Phys. J. D* **18**, 129 (2002).
- [36] A. Andre, L. M. Duan, and M. D. Lukin, *Phys. Rev. Lett.* **88**, 243602 (2002).
- [37] D. W. Berry and B. C. Sanders, *Phys. Rev. A* **66**, 012313 (2002).
- [38] S. Sinha, J. Emerson, N. Boulant, E. M. Fortunato, T. F. Havel, and D. G. Cory, *Quantum Inf. Proc.* **2**, 433 (2003).
- [39] J. M. Geremia, J. K. Stockton, and H. Mabuchi, *Phys. Rev. Lett.* **94**, 203002 (2005).
- [40] S. Choi and N. P. Bigelow, *Phys. Rev. A* **72**, 033612 (2005).
- [41] M. Takeuchi, S. Ichihara, T. Takano, M. Kumakura, T. Yabuzaki, and Y. Takahashi, *Phys. Rev. Lett.* **94**, 023003 (2005).
- [42] S. Yi and H. Pu, *Phys. Rev. A* **73**, 023602 (2006).
- [43] G.-B. Jo, Y. Shin, S. Will, T. A. Pasquini, M. Saba, W. Ketterle, D. E. Pritchard, M. Vengalattore, and M. Prentiss, *Phys. Rev. Lett.* **98**, 030407 (2007).
- [44] T. Fernholz, H. Krauter, K. Jensen, J. F. Sherson, A. S. Sorensen, and E. S. Polzik, *Phys. Rev. Lett.* **101**, 073601 (2008).
- [45] J. Esteve, C. Gross, A. Weller, S. Giovanazzi, and M. K. Oberthaler, *Nature (London)* **455**, 1216 (2008).
- [46] L. Pezze and A. Smerzi, *Phys. Rev. Lett.* **102**, 100401 (2009).
- [47] Y. Li, Y. Castin, and A. Sinatra, *Phys. Rev. Lett.* **100**, 210401 (2008).
- [48] T. Takano, M. Fuyama, R. Namiki, and Y. Takahashi, *Phys. Rev. Lett.* **102**, 033601 (2009).
- [49] C. Gross, T. Zibold, E. Nicklas, J. Esteve, and M. K. Oberthaler, *Nature (London)* **464**, 1165 (2010).
- [50] I. D. Leroux, M. H. Schleier-Smith, and V. Vuletic, *Phys. Rev. Lett.* **104**, 073602 (2010).
- [51] J. D. Sau, S. R. Leslie, M. L. Cohen, and D. M. Stamper-Kurn, *New J. Phys.* **12**, 085011 (2010).
- [52] F. Benatti, R. Floreanini, and U. Marzolino, *J. Phys. B* **44**, 091001 (2011).
- [53] Z. Chen, J. G. Bohnet, S. R. Sankar, J. Dai, and J. K. Thompson, *Phys. Rev. Lett.* **106**, 133601 (2011).
- [54] Y. C. Liu, Z. F. Xu, G. R. Jin, and L. You, *Phys. Rev. Lett.* **107**, 013601 (2011).
- [55] C. D. Hamley, C. S. Gerving, T. M. Hoang, E. M. Bookjans, and M. S. Chapman, *Nat. Phys.* **8**, 305 (2012).
- [56] B. Julia-Diaz, T. Zibold, M. K. Oberthaler, M. Mele-Messeguer, J. Martorell, and A. Polls, *Phys. Rev. A* **86**, 023615 (2012).
- [57] E. Yukawa, G. J. Milburn, C. A. Holmes, M. Ueda, and K. Nemoto, *Phys. Rev. A* **90**, 062132 (2014).
- [58] T. Opatrny, M. Kolar, and K. K. Das, *Phys. Rev. A* **91**, 053612 (2015).
- [59] T. Opatrny, *Phys. Rev. A* **91**, 053826 (2015).
- [60] M. S. Rudner, L. M. K. Vandersypen, V. Vuletic, and L. S. Levitov, *Phys. Rev. Lett.* **107**, 206806 (2011).
- [61] K. R. A. Hazzard, S. R. Manmana, M. Foss-Feig, and A. M. Rey, *Phys. Rev. Lett.* **110**, 075301 (2013).
- [62] We note however that the possibility of squeezing a single atomic spin with $J > 1/2$ was suggested by Wineland *et al.* [[19], [20]].
- [63] S. Chaudhury, S. Merkel, T. Herr, A. Silberfarb, I. H. Deutsch, and P. S. Jessen, *Phys. Rev. Lett.* **99**, 163002 (2007).
- [64] R. Auccaise, A. G. Araujo-Ferreira, R. S. Sarthour, I. S. Oliveira, T. J. Bonagamba, and I. Roditi, *Phys. Rev. Lett.* **114**, 043604 (2015).
- [65] S. M. Rochester, M. P. Ledbetter, T. Zigdon, A. D. Wilson-Gordon, and D. Budker, *Phys. Rev. A* **85**, 022125 (2012).
- [66] M. Auzinsh, D. Budker, D. F. Kimball, S. M. Rochester, J. E. Stalnaker, A. O. Sushkov, and V. V. Yashchuk, *Phys. Rev. Lett.* **93**, 173002 (2004).
- [67] P. Cappellaro and M. D. Lukin, *Phys. Rev. A* **80**, 032311 (2009).
- [68] V. Shah, G. Vasilakis, and M. V. Romalis, *Phys. Rev. Lett.* **104**, 013601 (2010).
- [69] W. Wasilewski, K. Jensen, H. Krauter, J. J. Renema, M. V. Balabas, and E. S. Polzik, *Phys. Rev. Lett.* **104**, 133601 (2010).
- [70] R. J. Sewell, M. Koschorreck, M. Napolitano, B. Dubost, N. Behbood, and M. W. Mitchell, *Phys. Rev. Lett.* **109**, 253605 (2012).
- [71] S. Y. Lee, M. Niethammer, and J. Wrachtrup, *Phys. Rev. B* **92**, 115201 (2015).
- [72] M. Gärttner, J. J. Olmiste, P. Schmelcher, and R. Gonzalez-Ferez, *Mol. Phys.* **111**, 1865 (2013).
- [73] M. Lara, B. L. Lev, and J. L. Bohn, *Phys. Rev. A* **78**, 033433 (2008).
- [74] B. K. Stuhl, M. Yeo, B. C. Sawyer, M. T. Hummon, and J. Ye, *Phys. Rev. A* **85**, 033427 (2012).
- [75] M. Bhattacharya, Z. Howard, and M. Kleinert, *Phys. Rev. A* **88**, 012503 (2013).
- [76] J. L. Bohn and G. Quemener, *Mol. Phys.* **111**, 1931 (2013).
- [77] S. C. Doret, J. M. Amini, K. Wright, C. Volin, T. Killian, A. Ozakin, D. Denison, H. Hayden, C. S. Pai, R. E. Slusher, and A. W. Harter, *New J. Phys.* **14**, 073012 (2012).
- [78] J. J. Sakurai, *Modern Quantum Mechanics* (Addison-Wesley, Reading, MA, 2010).
- [79] A. G. Rojo, *Phys. Rev. A* **68**, 013807 (2003).
- [80] J. Vidal, G. Palacios, and C. Aslangul, *Phys. Rev. A* **70**, 062304 (2004).
- [81] G.-R. Jin and S. W. Kim, *Phys. Rev. A* **76**, 043621 (2007).
- [82] G.-R. Jin and S. W. Kim, *Phys. Rev. Lett.* **99**, 170405 (2007).
- [83] K. Maeda, M. L. Wall, and L. D. Carr, *New J. Phys.* **17**, 045014 (2015).